ACS Energy LETTERS

http://pubs.acs.org/journal/aelccp

VIEWPOINT

Ionic Losses and Gains in Perovskite Solar Cells: Impact on Efficiency and Stability

Cite This: *ACS Energy Lett.* 2025, 10, 4849−4855

Read Online

ACCESS | Metrics & More | Article Recommendations | Supporting Information

Mobile ionic charges can significantly affect the performance of perovskite solar cells (PSCs) in terms of power conversion efficiency (PCE), as well as stability if their density changes over time. However, assigning performance losses during aging to ionic losses requires a reference point which is independent of the mobile ion density. In this Viewpoint we discuss, using drift-diffusion simulations, how the mobile ion density can affect the PCE obtained from a fast $J-V$ scan when the preconditioning voltage does not match the voltage at which the ionic space charge vanishes. Depending on device properties, this misalignment can induce relative performance gains thanks to mobile ions and lead to an overestimation of the ionic loss. Taking into account the interplay between ion density and competing recombination pathways is crucial for the loss and degradation analysis of PSCs.

Ionic Losses as the PCE Difference between the Fast and Slow $J-V$ Scan. Over aging of PSCs, the PCE measured fast from an open-circuit voltage (V_{OC}) precondition often shows far less degradation than the stabilized PCE.[1−3] This has been attributed to the slow response and electric field screening effect of mobile ions,[4] which aggravates as the ion density increases over time, affecting mainly the short-circuit current (J_{SC}).[1,2,5−8] Recent studies using scan rate-dependent $J-V$ measurements and drift-diffusion simulations have shown that the PCE from a fast $J-V$ scan starting with a V_{OC} precondition, can reflect the stability of a device where ionic screening is prevented.[2,7,9] If the effective built-in voltage (V_{bi}) in the perovskite layer is high enough that $V_{OC} \approx V_{bi}$, fixing the ionic distribution for the V_{OC} value can approximate what would happen in an equivalent device without ions.[10,11] This is because the ionic charge should be mostly spread throughout the bulk, where negative and positive ions would compensate each other. Thus, the PCE from a fast $J-V$ scan where ions have no time to respond (starting from a precondition around V_{OC}) can be used as a reference point from which to measure the ionic loss as

$$\text{Ionic loss} := \Delta\text{PCE} = \text{PCE}_{\text{fast}} - \text{PCE}_{\text{stabilized}} \quad (1)$$

Any losses also present in the preconditioned PCE_{fast} can then be attributed to non-ionic losses, e.g., increase in nonradiative recombination.[2,3,9] Nonetheless, analyzing performance losses this way across all PSCs in general requires caution, as ions may not always be the culprit.[12,13] If the electrostatic effect of the ion density N_{ion} alone can significantly decrease the stabilized PCE of a device, as observed during degradation,[2] it means that diffusive electron and hole transport is not efficient and the device requires the assistance of the bulk electric field to extract the photogenerated charges.[14] In short, a high sensitivity of the J_{SC} to N_{ion} alone requires pre-existing recombination pathways which compete with diffusion-dominated transport.[15] However, initial ion densities in solution-processed perovskites are expected to be high,[16,17] meaning that substantial field screening could in many cases be present from the start. Thus, it is arguable whether high-efficiency PSCs should be generally so sensitive to the electrostatic effect of N_{ion} alone, or if first the recombination rate should increase sufficiently for the available N_{ion} to amplify any losses. However, the interplay between ions and recombination, determining whether their presence amplifies or minimizes losses relative to an ion-free device, depends strongly on the energetic configuration of the PSC.[12,13]

Energetic Alignment Dominates Ionic Impact on PCE. Figure 1a,b shows two energetic configurations for comparison (simulation parameters are provided in Table 1). In the first case, the high difference in the work function of the electrodes and aligned charge transport layers (CTLs) result in a high V_{bi} in the perovskite layer. As shown in Figure 1a, the "ion-free" voltage nearly coincides with the 1 sun-V_{OC} of the device (1.2 V), lying just above it (1.25 V). However, lowering the work function difference and introducing an energy offset with the CTLs shifts the "ion-free" voltage significantly below V_{OC} (0.85 V), as shown in Figure 1b. This difference critically affects the accuracy of disentangling ionic from non-ionic losses using the described method (eq 1). For context, "ion-free" voltages for high efficiency p-i-n PSCs were recently reported in ref 18, comparing various perovskite compositions and self-assembled monolayers (SAMs); resulting values range from 0.6 to 1.0 V, consistently below the V_{OC} of the devices (by different amounts).

Figure 1c shows simulated band diagrams at short circuit for the low V_{bi} model, with varying the ion density N_{ion}. The

Received: August 1, 2025
Accepted: August 25, 2025
Published: September 8, 2025

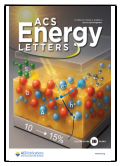

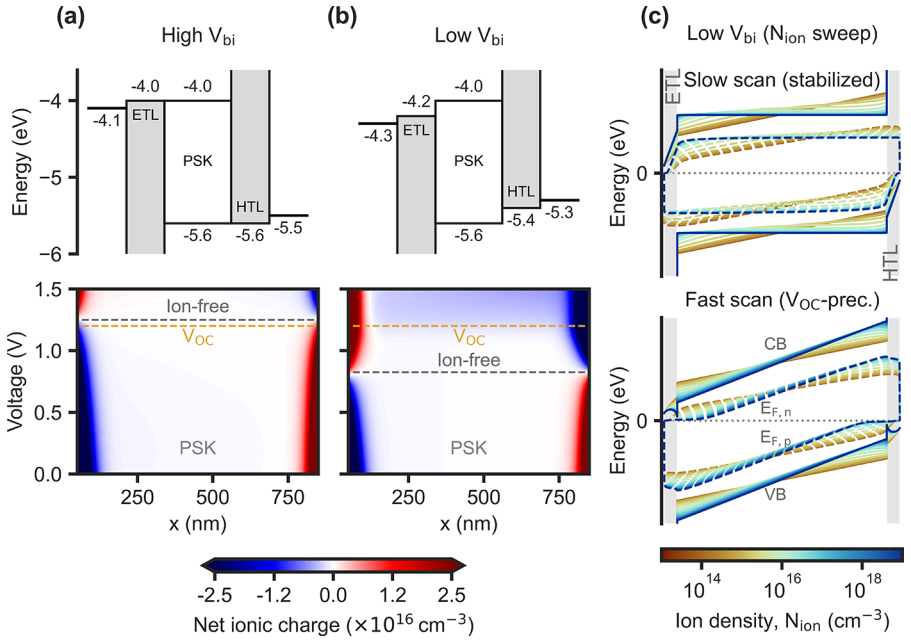

Figure 1. Energy band configurations for PSC with (a) aligned CTLs and high V_{bi} and (b) offset CTLs and lower V_{bi}, showing the respective net ionic charge profiles under different applied voltages, for an input N_{ion} of 10^{17} cm^{-3}. The dashed lines highlight the 1 sun-V_{OC} and the voltage where the net ionic charge has its minimum ("ion-free"). (c) Simulated band diagrams at short circuit for the low V_{bi} case with varying N_{ion}, showing the stabilized condition and the profiles where the ionic charge is instead fixed at the V_{OC} value in (b).

Table 1. Parameters Used in the Simplified PSC Model in Setfos[a]

Parameter	ETL	PSK	HTL
Thickness, d [nm]	50	800	50
Valence band edge, VB [eV]	-7.5	-5.6	-5.4
Conduction band edge, CB [eV]	-4.2	-4.0	-2.1
Density of states, DOS_{VB} [cm^{-3}]	10^{19}	10^{19}	10^{19}
Density of states, DOS_{CB} [cm^{-3}]	10^{19}	10^{19}	10^{19}
Electron mobility, μ_n [cm^2 V^{-1} s^{-1}]	10^{-3}	1/Varied (**Sweep 1**)	10^{-3}
Hole mobility, μ_p [cm^2 V^{-1} s^{-1}]	10^{-3}	1/Varied (**Sweep 1**)	10^{-3}
Anion mobility, μ_a [cm^2 V^{-1} s^{-1}]		Uniform & static	
Cation mobility, μ_c [cm^2 V^{-1} s^{-1}]		5×10^{-10}	
Dielectric constant, ε	5	25	5
Anion density, N_a [cm^{-3}]		**Sweep**	
Cation density, N_c [cm^{-3}]		**Sweep**	
Bimolecular rec. prefactor, β_γ [cm^3 s^{-1}]		10^{-10}	
SRH lifetimes, τ_n and τ_p [ns]		200 (Sweep 1)/∞ (Sweep 2)	
Interface rec. velocity, $v_{int,SRH}$ [ms^{-1}]		0.1 (Sweep 1)/Varied (**Sweep 2**)	

[a]The electrode work functions are given in Figure 1. ETL and HTL denote the electron and hole transport layers, respectively. The energetic alignment corresponds to the lower V_{bi} case. The energy level values for the high V_{bi} case are given in Figure 1a. The generation rate in perovskite is calculated using AM1.5G spectra, the complex refractive index of $MAPbI_3$ and common CTL materials from the Setfos database.

lowest N_{ion} considered is sufficiently low to be effectively the same as an equivalent device without ions.

At short circuit, the reduced band tilt in the perovskite shows that the electric field decreases due to the ionic space charge accumulated at the contacts. For the high V_{bi} case, fixing the ionic charge at the V_{OC} distribution prevents the screening effect, restoring the "ion-free" band diagram. However, for the low V_{bi} case, ions are not any more compensated in the bulk at V_{OC}, and the ionic space charge layers invert polarity relative to the short circuit distribution (Figure 1b); as a result, increasing N_{ion} now tends to strengthen the bulk electric field, as seen by the steeper tilt of the bands. This introduces a key implication: the fast J–V scan from a V_{OC}-precondition is no longer independent of N_{ion}, so it cannot be used as reference to classify losses as ionic or non-ionic.

Ideal Case (High V_{bi}): Ionic Losses = ΔPCE. To discuss the interplay between ionic and electronic effects, we look at a rising N_{ion} with surface recombination as an example, which is a known limiting loss in PSCs.[19] Figure 2 shows simulated PCE values for varying the interface Shockley-Read-Hall (SRH) recombination velocity ($v_{int,SRH}$) with varying levels of N_{ion}, for the high V_{bi} case (Figure 1a) where the initial V_{OC} (1.2 V) roughly matches the "ion-free" voltage. The simulation parameters are specified in Table 1. The difference between the stabilized PCE (Figure 2a) and the preconditioned PCE where the ionic distribution is always fixed for the initial V_{OC} value (Figure 2b), is shown in Figure 2c. An example degradation pathway where both N_{ion} and $v_{int,SRH}$ increase is shown by the gray dashed lines, and plotted in Figure 2d. As expected, in this case the analysis based on eq 1 works nicely, since the preconditioned PCE mostly follows the ion-free trace, which directly corresponds to the non-ionic loss. For this example, the ionic loss (eq 1) would be only slightly underestimated, due to the slight misalignment between the precondition and the "ion-free" value in Figure 1b. Ideally, the preconditioned PCE in Figure 2b would be constant vertically, for the fast scan to be fully independent of N_{ion}. Then, if ΔPCE

https://doi.org/10.1021/acsenergylett.5c02435
ACS Energy Lett. 2025, 10, 4849−4855

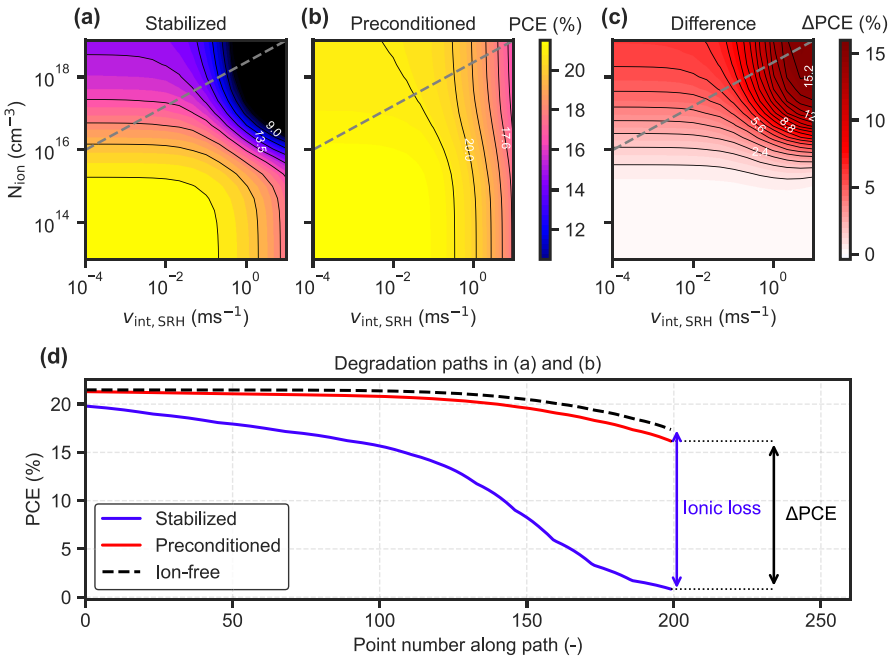

Figure 2. Simulation for PSC with aligned CTLs and high V_{bi}. (a)−(c) Simulated PCE maps as a function of N_{ion} and interface recombination velocity $v_{int,SRH}$, from stabilized and preconditioned J−V curves. (d) Example degradation pathways as shown by the dashed lines in (a) and (b), where both N_{ion} and $v_{int,SRH}$ increase.

is not constant horizontally (Figure 2c), it means the ionic loss is being amplified by a deteriorated electronic property. This is further illustrated by a sweep of the CTL mobility (Figure S1 in the Supporting Information), demonstrating how a limited charge mobility in the CTLs[20,21] can also result in an increased ionic loss. Furthermore, if Figure 2b is not mostly constant vertically, then the ionic loss does not correspond to ΔPCE.

Low V_{bi} Case: Ionic Loss ≠ ΔPCE. Depending on the energy level alignment, V_{OC} can be higher than the effective V_{bi},[11,13] leading to ionic space charge accumulation also at V_{OC} (Figure 1b). With effective V_{bi} we mean the potential drop in the perovskite, which can be lower than the work function difference of the contacts due to high potential drop in the CTLs, especially when they are undoped and have a low dielectric constant. If there is ionic accumulation at the precondition used for the fast scan, the resulting J_{SC} may then benefit from the increased electric field in the bulk provided by the ionic space charge, which increases with N_{ion} as shown in Figure 1c. Such accumulation can also have a negative effect depending on the device properties and available recombination pathways, potentially leading to inverted hysteresis,[22,23] which could result in a negative ΔPCE.

To exemplify how ionic accumulation may affect the analysis, we look at the low V_{bi} case, where the "ion-free" voltage is lower than V_{OC}. Two scenarios are compared; in the first one, denoted as "Sweep 1", the electronic mobility in perovskite μ_{PSK} is varied for different N_{ion} (mimicking degradation in the charge transport properties of the perovskite), with unmodified bulk- and interface-SRH recombination parameters. In the second scenario ("Sweep 2") there is no bulk-SRH, and only the interface SRH-recombination velocity $v_{int,SRH}$ is varied for different N_{ion} (as in the first example above), keeping a constant μ_{PSK}. The simulated performance metrics of the PSC under varying N_{ion} are shown in Figure S2 in the Supporting Information. For Sweep 1, reducing μ_{PSK} provides a higher sensitivity to changes in the electric field. At any value of μ_{PSK}, the charge collection efficiency drops due to the screening effect of N_{ion}, reducing the J_{SC}. However, the V_{OC} and fill factor (FF) show an inverse dependence and actually benefit from the ionic space charge, as explained in refs.[12,13] As a result, while the PCE tends to reduce with decreasing μ_{PSK}, it first increases with N_{ion} until μ_{PSK} is sufficiently low. For Sweep 2, a similar trend can be observed with $v_{int,SRH}$. Here, the initial PCE (low $v_{int,SRH}$) is also initially higher with enhanced N_{ion}, again due to the increase of V_{OC}[24] and FF dominating over the loss in J_{SC}. The trend in PCE with N_{ion} then inverts once $v_{int,SRH}$ is sufficiently high.

Thus, in simulations the stabilized PCE of a PSC is not always higher in the absence of mobile ions, since for instance, they can enhance the cell's tolerance to energetic offsets with the transport layers.[12,13] Figure 3 compares how the PCE differs from the stabilized one when preconditioning above the "ion-free" voltage and fixing the ions in the resulting distribution. The preconditioned PCE again corresponds to the fast scan PCE measured in experiment, where ions have no time to respond. The effect of ionic accumulation at the precondition voltage (1.2 V) is not independent of N_{ion}, as the PCE is not constant vertically in Figure 3b. For both the μ_{PSK} sweep (Figure 3a−c) and the $v_{int,SRH}$ sweep (Figure 3d−f) the preconditioned PCE is always higher than the stabilized one, as in the first example above. This results in a positive ΔPCE (eq 1) which increases with N_{ion}, especially for high recombination rates, either due to the low μ_{PSK} or to the high $v_{int,SRH}$. However, ΔPCE tends to saturate at moderately high N_{ion} once the electric field is completely screened, as seen by the mostly vertical lines in Figure 3c where $N_{ion} \gtrsim 10^{17}$ cm^{-3}. Most importantly, the preconditioned PCE becomes significantly more tolerant to higher recombination rates by increasing N_{ion}, as seen by the horizontal shift of the PCE contours in Figure 3b,e in the high N_{ion} range. The ΔPCE maps in Figure 3c,f show that, along a horizontal path at constant N_{ion}, ΔPCE

https://doi.org/10.1021/acsenergylett.5c02435
ACS Energy Lett. 2025, 10, 4849−4855

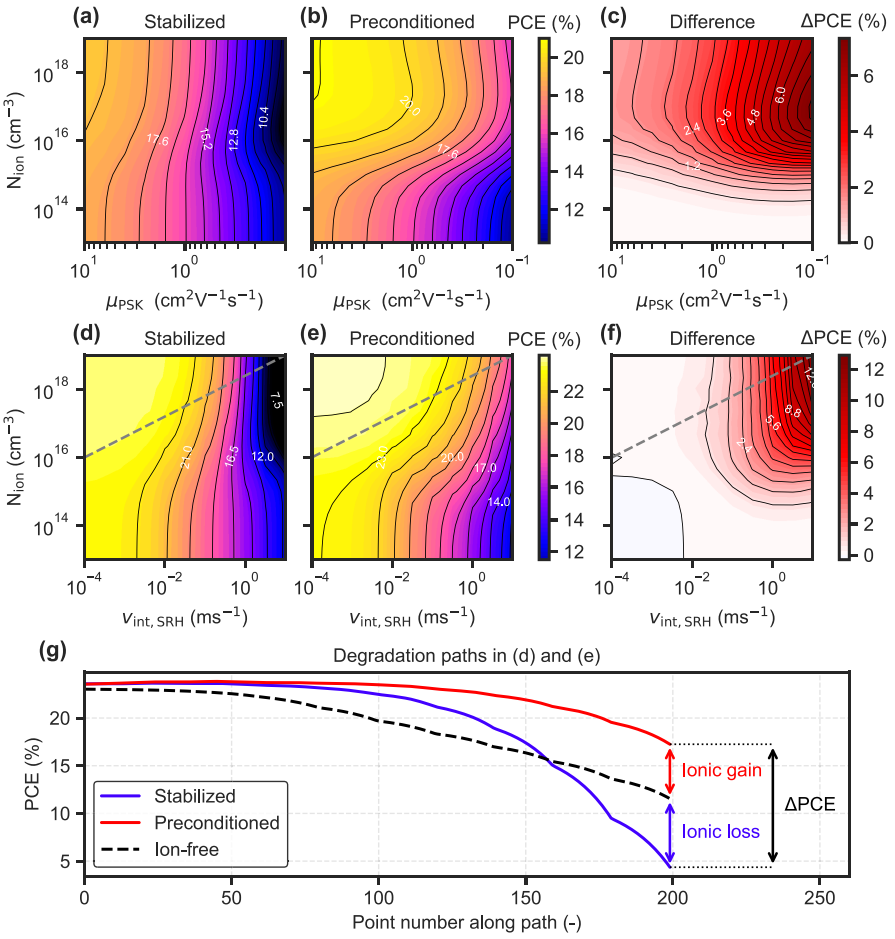

Figure 3. Simulation for PSC with energy offset at CTLs and lower V_{bi}. (a)−(c) Simulated PCE maps as a function of N_{ion} and electronic mobility in perovskite μ_{PSK}. (a) Stabilized PCE (slow J−V scan). (b) PCE with a fixed ionic distribution preconditioned at 1.2 V (fast J−V scan from a precondition around the initial V_{OC}). (c) Difference between the preconditioned and stabilized PCEs. (d)−(f) Simulated PCE maps as a function of N_{ion} and interface recombination velocity $v_{int,SRH}$, from stabilized and preconditioned J−V curves. (g) Example degradation pathways as shown by the dashed lines in (d) and (e), where both N_{ion} and $v_{int,SRH}$ increase.

increases significantly due to a change in electronic properties that ions amplify. This is similar to the analysis of J−V hysteresis, where a change in hysteresis does not necessarily indicate a change in ionic properties.[25] Therefore, in practice it is important to complement ΔPCE analysis with techniques that can identify changes in N_{ion}.[2,26]

For the $v_{int,SRH}$ sweep in Figure 3d−f, an example degradation pathway is drawn as a gray diagonal line across the $v_{int,SRH}$−N_{ion} space. This would roughly correspond to a situation where both the ion density in perovskite and the quality of the interfaces are degrading over time. The PCE difference between the stabilized and preconditioned performance is shown in Figure 3g, which highlights how there can be an ionic gain relative to the ion-free performance. The trace of the ion-free device with increasing $v_{int,SRH}$ can be assigned to the non-ionic loss, i.e., the degradation resulting from $v_{int,SRH}$ alone in an equivalent device without ions. In the initial stages, there is a higher PCE for both the stabilized and the preconditioned curves, which means that there would be no real ionic loss at this point, despite the PCE difference that would be measured between a fast and a slow J−V scan. An ionic loss can be seen in the final stages, where the stabilized curve decreases below the ion-free trace. However, the ΔPCE between the preconditioned and stabilized traces still comprises both a gain and a loss relative to the ion-free performance, so the ionic loss from eq 1 would be overestimated. As a result, ionic losses can only be quantified correctly if the "ion-free" trace is known, as otherwise the PCE for a precondition around V_{OC} is also dependent on N_{ion}. A PCE decrease where V_{OC} is mostly unchanged and a decreasing J_{SC} dominates is not either directly indicative of ionic changes alone, since in this case an increasing N_{ion} could compensate the radiative yield loss at V_{OC} that would be expected from a rising $v_{int,SRH}$. In simulations, this can always be easily checked, and the equivalent device performance without ions should be reported when discussing an ionic loss. In experiment, fast J−V scans from the true "ion-free" precondition voltage (if it exists in practice and can be determined[11,13,18]) should be used as the reference PCE trace over aging.

"Ion-Free" Voltage May Change during Degradation. As discussed above, ionic accumulation does not depend only on the potential originating from the work function difference between the electrodes, but also on the energetic offsets ΔE_{CTL} with the CTLs. So far we have considered an "ion-free" voltage which remains mostly unchanged over time, although it is possible that the degradation of CTLs, which often preludes that of the perovskite, could significantly shift this voltage over time. This could happen for instance, if the SAM in a p-i-n device degrades[27] and loses its dipole. Figure 4a depicts the

https://doi.org/10.1021/acsenergylett.5c02435
ACS Energy Lett. 2025, 10, 4849−4855

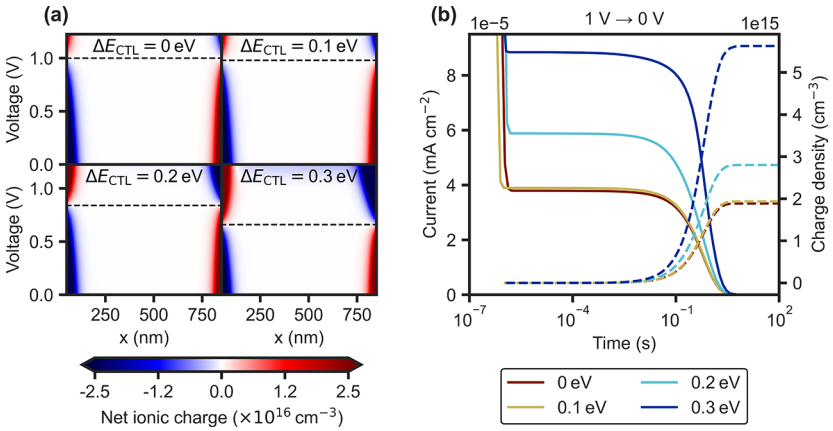

Figure 4. (a) Net ionic charge across the depth of the perovskite bulk (x) for different applied voltages and energy level offsets with the CTLs (ΔE_{CTL}), for an input density of 10^{17} cm^{-3}. The work function difference between the metal electrodes is kept constant at 1 eV. The "ion-free" voltage is marked as a dashed line for each case. (b) Transient dark current upon a sudden switch from 1 to 0 V, for the different ΔE_{CTL} configurations and cumulative ionic charge density using $N_{ion} = \int J(t)\, dt \frac{1}{q\, d_{PSK}}$.

simulated net ionic charge for different energetic offsets ΔE_{CTL}, where the dashed lines highlight the voltage at which most of the ionic charge is equilibrated in the bulk. Thus, using a constant preconditioning voltage for the fast scan PCE may result in a deviation from the "ion-free" condition, even if the starting one aligned. This would require a dynamic adaptation of the "ion-free" preconditioning voltage during aging.

Implications to Quantify Ion Density. Changed electronic properties can alter the level of ionic accumulation, for constant ionic properties (Figure 4a). This has implications for ΔPCE, but also for other measurements, as discussed next. To unravel how much of the performance changes originate from ionic electric field screening, it is important to quantify changes in N_{ion}. A useful approach is measuring the dark transient current upon a change from a preconditioning voltage (e.g., 1 to 0 V).[28] The drift of mobile ions after the sudden switch results in an external current which can be assigned to the ion density needed to screen the electric field,[29] although slow electrochemical processes (e.g., defect self-healing[30]) may also contribute to the measured current at longer time scales.[31] A rise in the transient current is expected to reflect a rise in N_{ion}. In experiment, the dark current can increase moderately[7,8] or even by orders of magnitude after stressing,[2,31,32] although it saturates earlier in simulations.[26,33] Without looking at the details of the sensitivity of this technique, which have been investigated in refs 26, 29, and 33, we look briefly at the effect of a changing "ion-free" voltage on the transient current response. If the transient current is measured always from the same precondition, 1 V in this example, and the "ion-free" voltage is shifting during degradation, this will already affect the amount of ionic accumulation at the precondition (Figure 4a). Thus, a change of the energetic alignment directly leads to a significant change in the current response (Figure 4b), even if N_{ion} remains constant (10^{17} cm^{-3} in this example). Therefore, while changes in the transient current may reflect changes in the amount of ionic accumulation, the underlying cause may not always be clear as any changes in the internal field resulting from CTL degradation can also have a significant effect on the ion migration current.[33]

Disentangling Ionic and Non-ionic Losses. In simulations, high mobile ion densities which can screen the bulk electric field can in theory be mostly harmless for all device architectures, and even beneficial for some, as long as diffusion-dominated transport remains efficient. In this regard, it remains to be answered whether ionic and recombination properties can in practice remain so independent as done in simulations, or whether they are linked to a degree that preventing degradation of electronic properties requires mostly unchanged ionic properties also.[34] The analysis of PCE degradation in PSCs should account for the interplay between different parameters, as illustrated here by the electrostatic influence of different ion densities on varying levels of competing recombination sources. In practice, electrochemical processes will also play a key role,[35] determining the transient generation of ionic defects (and potential self-annihilation enabling reversibility),[30] the mobility of those defects in different charge states,[36] as well as their direct coupling to charge trapping and recombination. While it remains important to explore further experimental observations which require explicit ionic-electronic interactions in drift-diffusion models,[37] simulations that consider only the electrostatic interaction of ions have so far reproduced many complex experimental trends successfully, and remain an important tool to understand the device physics of mixed ionic-electronic PSCs.

To summarize, the PCE difference (ΔPCE) between a fast and a slow (stabilized) $J-V$ scan does not directly correspond to the ionic loss if there is ionic accumulation at the preconditioning voltage used for the fast scan. This point is important to consider regardless of whether the device benefits or suffers from the presence of mobile ions. While mobile ions can surely have a detrimental effect on PSCs, care should be taken not to blame them directly without sufficient evidence that the equivalent device without ions would perform better. In addition, non-ion-related parameters may amplify ionic losses; changes in electronic properties can increase ΔPCE, although all ionic parameters remain unchanged. Therefore, combining degradation analysis with measurements to probe any changes in ion density remains important. The fast PCE from a V_{OC} precondition, which can sometimes be characteristic of an "ionic gain", should not be thought of as the performance of the equivalent device without ions, if the voltage at which ions are mostly compensated in the bulk is not known. Additionally, this value may also shift during degradation, which would require a dynamic adaptation of the preconditioning voltage used for the fast $J-V$ scan, in order to

https://doi.org/10.1021/acsenergylett.5c02435
ACS Energy Lett. 2025, 10, 4849−4855

properly disentangle ionic and non-ionic losses. Experimentally, it remains important to explore further characterization methods which can be used to determine the "ion-free" or "field-free" voltage and use them for degradation analysis. Taking this into account should help to establish a clearer picture of how mobile ions affect the efficiency and stability of PSCs.

Miguel A. Torre Cachafeiro orcid.org/0009-0004-6907-9826

Wolfgang Tress orcid.org/0000-0002-4010-239X

■ ASSOCIATED CONTENT

Supporting Information

The Supporting Information is available free of charge at https://pubs.acs.org/doi/10.1021/acsenergylett.5c02435.

Additional simulations (PDF)

■ AUTHOR INFORMATION

Complete contact information is available at: https://pubs.acs.org/10.1021/acsenergylett.5c02435

Notes

Views expressed in this Viewpoint are those of the author and not necessarily the views of the ACS.

The authors declare no competing financial interest.

■ ACKNOWLEDGMENTS

This research received funding from the European Union's Horizon 2020 research and innovation program under grant agreement no. 851676 (ERC StGrt).

■ REFERENCES

(1) Tress, W.; Marinova, N.; Moehl, T.; Zakeeruddin, S. M.; Nazeeruddin, M. K.; Grätzel, M. Understanding the rate-dependent J−V hysteresis, slow time component, and aging in CH 3 NH 3 PbI 3 perovskite solar cells: the role of a compensated electric field. *Energy Environ. Sci.* **2015**, *8*, 995−1004.

(2) Thiesbrummel, J.; Shah, S.; Gutierrez-Partida, E.; Zu, F.; Peña-Camargo, F.; Zeiske, S.; Diekmann, J.; Ye, F.; Peters, K. P.; Brinkmann, K. O.; et al. Ion-induced field screening as a dominant factor in perovskite solar cell operational stability. *Nature Energy* **2024**, *9*, 664−676.

(3) Rombach, F. M.; Dasgupta, A.; Kober-Czerny, M.; Jin, H.; Ball, J. M.; Smith, J. A.; Farrar, M. D.; Snaith, H. J. Disentangling degradation pathways of narrow bandgap lead-tin perovskite material and photovoltaic devices. *Nat. Commun.* **2025**, *16*, 5450.

(4) Richardson, G.; O'Kane, S. E.; Niemann, R. G.; Peltola, T. A.; Foster, J. M.; Cameron, P. J.; Walker, A. B. Can slow-moving ions explain hysteresis in the current−voltage curves of perovskite solar cells? *Energy Environ. Sci.* **2016**, *9*, 1476−1485.

(5) Thiesbrummel, J.; Le Corre, V. M.; Peña-Camargo, F.; Perdigón-Toro, L.; Lang, F.; Yang, F.; Grischek, M.; Gutierrez-Partida, E.; Warby, J.; Farrar, M. D.; et al. Universal current losses in perovskite solar cells due to mobile ions. *Adv. Energy Mater.* **2021**, *11*, No. 2101447.

(6) Moia, D. More ions in, less power out. *Nature Energy* **2024**, *9*, 633−634.

(7) Seid, B. A.; Ozen, S.; Castro-Mendez, A.-F.; Neher, D.; Stolterfoht, M.; Lang, F. Mitigating Mobile-Ion-Induced Instabilities and Performance Losses in 2D Passivated Perovskite Solar Cells. *Adv. Mater.* **2025**, *37*, No. 2501588.

(8) Scheler, F.; Mariotti, S.; Mantione, D.; Shah, S.; Menzel, D.; Köbler, H.; Simmonds, M.; Gries, T. W.; Kurpiers, J.; Škorjanc, V.; et al. Correlation of Band Bending and Ionic Losses in 1.68 eV Wide Band Gap Perovskite Solar Cells. *Adv. Energy Mater.* **2025**, *15*, No. 2404726.

(9) Shah, S.; Yang, F.; Köhnen, E.; Ugur, E.; Khenkin, M.; Thiesbrummel, J.; Li, B.; Holte, L.; Berwig, S.; Scherler, F.; et al. Impact of Ion Migration on the Performance and Stability of Perovskite-Based Tandem Solar Cells. *Adv. Energy Mater.* **2024**, *14*, No. 2400720.

(10) Le Corre, V. M.; Diekmann, J.; Pena-Camargo, F.; Thiesbrummel, J.; Tokmoldin, N.; Gutierrez-Partida, E.; Peters, K. P.; Perdigón-Toro, L.; Futscher, M. H.; Lang, F.; et al. Quantification of efficiency losses due to mobile ions in perovskite solar cells via fast hysteresis measurements. *Solar RRL* **2022**, *6*, No. 2100772.

(11) Hill, N. S.; Cowley, M. V.; Gluck, N.; Fsadni, M. H.; Clarke, W.; Hu, Y.; Wolf, M. J.; Healy, N.; Freitag, M.; Penfold, T. J.; et al. Ionic accumulation as a diagnostic tool in perovskite solar cells: characterizing band alignment with rapid voltage pulses. *Adv. Mater.* **2023**, *35*, No. 2302146.

(12) Córdoba, M.; Taretto, K. Insight into the dependence of Photovoltaic Performance on Interfacial Energy Alignment in Solar cells with Mobile ions. *Solar RRL* **2024**, *8*, No. 2300742.

(13) Hart, L. J.; Angus, F. J.; Li, Y.; Khaleed, A.; Calado, P.; Durrant, J. R.; Djurišić, A. B.; Docampo, P.; Barnes, P. R. More is different: mobile ions improve the design tolerances of perovskite solar cells. *Energy Environ. Sci.* **2024**, *17*, 7107−7118.

(14) Kirchartz, T.; Bisquert, J.; Mora-Sero, I.; Garcia-Belmonte, G. Classification of solar cells according to mechanisms of charge separation and charge collection. *Phys. Chem. Chem. Phys.* **2015**, *17*, 4007−4014.

(15) Wu, N.; Walter, D.; Fell, A.; Wu, Y.; Weber, K. The impact of mobile ions on the steady-state performance of perovskite solar cells. *J. Phys. Chem. C* **2020**, *124*, 219−229.

(16) Walsh, A.; Scanlon, D. O.; Chen, S.; Gong, X.; Wei, S.-H. Self-regulation mechanism for charged point defects in hybrid halide perovskites. *Angew. Chem., Int. Ed.* **2015**, *54*, 1791−1794.

(17) Walsh, A.; Stranks, S. D. Taking control of ion transport in halide perovskite solar cells. *ACS Energy Letters* **2018**, *3*, 1983−1990.

(18) Angus, F. J.; Yiu, W. K.; Mo, H.; Leung, T. L.; Ali, M. U.; Li, Y.; Wang, J.; Ho-Baillie, A. W.; Cooke, G.; Djurisic, A. B.; et al. Understanding the Impact of SAM Fermi Levels on High Efficiency pin Perovskite Solar Cells. *J. Phys. Chem. Lett.* **2024**, *15*, 10686−10695.

(19) Wolff, C. M.; Caprioglio, P.; Stolterfoht, M.; Neher, D. Nonradiative recombination in perovskite solar cells: the role of interfaces. *Adv. Mater.* **2019**, *31*, No. 1902762.

(20) Le Corre, V. M.; Stolterfoht, M.; Perdigon Toro, L.; Feuerstein, M.; Wolff, C.; Gil-Escrig, L.; Bolink, H. J.; Neher, D.; Koster, L. J. A. Charge transport layers limiting the efficiency of perovskite solar cells: how to optimize conductivity, doping, and thickness. *ACS Applied Energy Materials* **2019**, *2*, 6280−6287.

(21) Akel, S.; Wang, Y.; Yan, G.; Rau, U.; Kirchartz, T. Charge Carrier Collection Losses in Lead-Halide Perovskite Solar Cells. *Adv. Energy Mater.* **2024**, *14*, No. 2401800.

(22) Shen, H.; Jacobs, D. A.; Wu, Y.; Duong, T.; Peng, J.; Wen, X.; Fu, X.; Karuturi, S. K.; White, T. P.; Weber, K.; et al. Inverted hysteresis in CH3NH3PbI3 solar cells: role of stoichiometry and band alignment. *journal of physical chemistry letters* **2017**, *8*, 2672−2680.

(23) Jacobs, D. A.; Wu, Y.; Shen, H.; Barugkin, C.; Beck, F. J.; White, T. P.; Weber, K.; Catchpole, K. R. Hysteresis phenomena in perovskite solar cells: the many and varied effects of ionic accumulation. *Phys. Chem. Chem. Phys.* **2017**, *19*, 3094−3103.

(24) Deng, Y.; Xiao, Z.; Huang, J. Light-Induced Self-Poling Effect on Organometal Trihalide Perovskite Solar Cells for Increased Device Efficiency and Stability. *Adv. Energy Mater.* **2015**, *5*, No. 1500721.

(25) Tress, W. Metal Halide Perovskites as Mixed Electronic−Ionic Conductors: Challenges and Opportunities From Hysteresis to Memristivity. *journal of physical chemistry letters* **2017**, *8*, 3106−3114.

(26) Diekmann, J.; Peña-Camargo, F.; Tokmoldin, N.; Thiesbrummel, J.; Warby, J.; Gutierrez-Partida, E.; Shah, S.; Neher, D.; Stolterfoht, M. Determination of mobile ion densities in halide

perovskites via low-frequency capacitance and charge extraction techniques. *J. Phys. Chem. Lett.* **2023**, *14*, 4200−4210.
(27) Yu, X.; Sun, X.; Zhu, Z.; Li, Z. Stabilization Strategies of Buried Interface for Efficient SAM-Based Inverted Perovskite Solar Cells. *Angew. Chem., Int. Ed.* **2025**, *64*, No. e202419608.
(28) Game, O. S.; Buchsbaum, G. J.; Zhou, Y.; Padture, N. P.; Kingon, A. I. Ions matter: description of the anomalous electronic behavior in methylammonium lead halide perovskite devices. *Adv. Funct. Mater.* **2017**, *27*, No. 1606584.
(29) Diethelm, M.; Lukas, T.; Smith, J.; Dasgupta, A.; Caprioglio, P.; Futscher, M.; Hany, R.; Snaith, H. J. Probing ionic conductivity and electric field screening in perovskite solar cells: a novel exploration through ion drift currents. *Energy Environ. Sci.* **2025**, *18*, 1385−1397.
(30) Xu, Z.; Kerner, R. A.; Kronik, L.; Rand, B. P. Beyond ion migration in metal halide perovskites: toward a broader photoelectrochemistry perspective. *ACS Energy Letters* **2024**, *9*, 4645−4654.
(31) Torre Cachafeiro, M. A.; Comi, E. L.; Parayil Shaji, S.; Narbey, S.; Jenatsch, S.; Knapp, E.; Tress, W. Ion migration in mesoscopic perovskite solar cells: Effects on electroluminescence, open circuit voltage, and photovoltaic quantum efficiency. *Adv. Energy Mater.* **2025**, *15*, No. 2403850.
(32) Tayagaki, T.; Hirooka, S.; Kobayashi, H.; Yamamoto, K.; Murakami, T. N.; Yoshita, M. Ion-migration analysis of degradation caused by outdoor exposure and accelerated stress testing in perovskite solar cells. *Sol. Energy Mater. Sol. Cells* **2024**, *272*, No. 112879.
(33) Schmidt, M. C.; Ehrler, B. How Many Mobile Ions Can Electrical Measurements Detect in Perovskite Solar Cells? *ACS Energy Letters* **2025**, *10*, 2457−2460.
(34) Kim, G.-W.; Petrozza, A. Defect tolerance and intolerance in metal-halide perovskites. *Adv. Energy Mater.* **2020**, *10*, No. 2001959.
(35) Moia, D.; Maier, J. Ion transport, defect chemistry, and the device physics of hybrid perovskite solar cells. *ACS Energy Letters* **2021**, *6*, 1566−1576.
(36) Tyagi, V.; Pols, M.; Brocks, G.; Tao, S. Tracing Ion Migration in Halide Perovskites with Machine Learned Force Fields. *J. Phys. Chem. Lett.* **2025**, *16*, 5153−5159.
(37) Bertoluzzi, L.; Patel, J. B.; Bush, K. A.; Boyd, C. C.; Kerner, R. A.; O'Regan, B. C.; McGehee, M. D. Incorporating Electrochemical Halide Oxidation into Drift-Diffusion Models to Explain Performance Losses in Perovskite Solar Cells under Prolonged Reverse Bias. *Adv. Energy Mater.* **2021**, *11*, No. 2002614.

https://doi.org/10.1021/acsenergylett.5c02435
ACS Energy Lett. 2025, 10, 4849−4855

Supporting Information (SI): Ionic Losses and Gains in Perovskite Solar Cells: Impact on Efficiency and Stability

Miguel A. Torre Cachafeiro[1,2] and Wolfgang Tress*[1]

[1]Institute of Computational Physics, Zurich University of Applied Sciences (ZHAW), 8400 Winterthur, Switzerland
[2]Institut des Matériaux, École Polytechnique Fédérale de Lausanne (EPFL), 1015 Lausanne, Switzerland

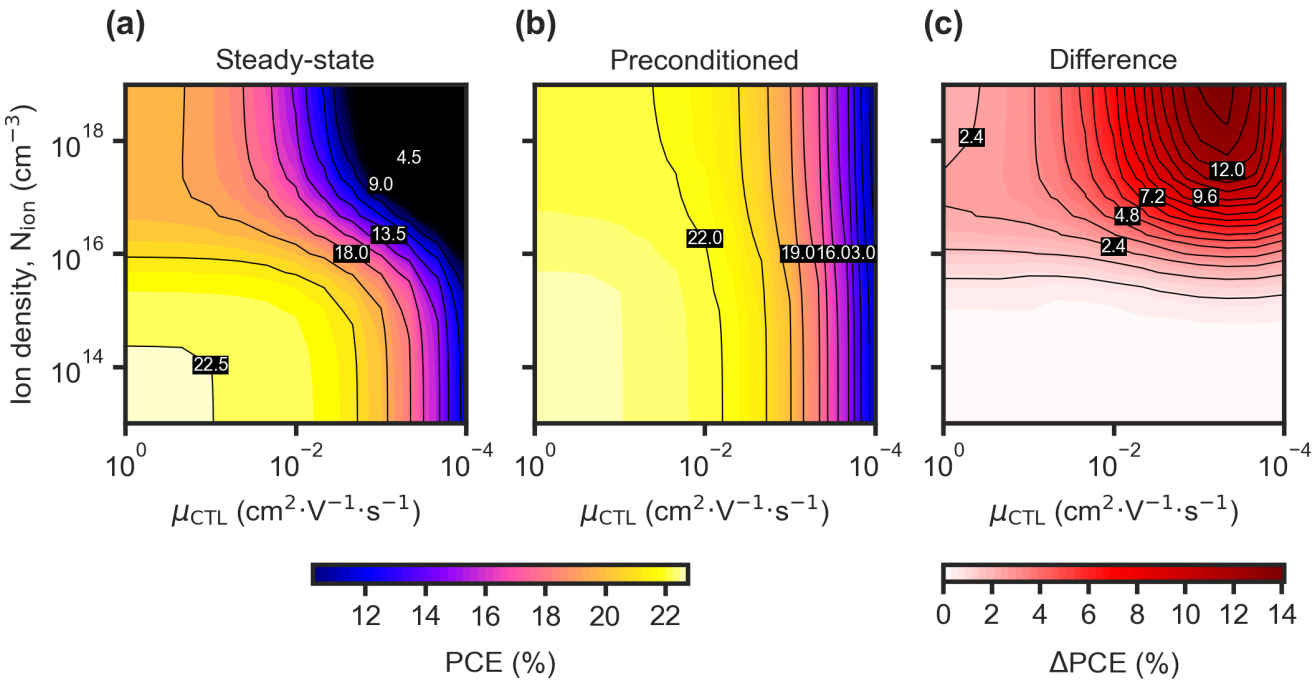

Figure S 1: Simulation for PSC with aligned CTLs and high V_{bi}. Charge transport layer-limited device, where the recombination rates are kept constant and only the mobility of electrons and holes in the CTLs (μ_{CTL}) is varied with N_{ion}. In this model the 'ion-free' voltage, where the absolute net ionic charge reaches a minimum, roughly coincides with V_{OC}. (a) Stabilized PCE and (b) preconditioned (1.2 V) PCE. (c) PCE difference between the preconditioned and stabilized values.

*Email: wolfgang.tress@zhaw.ch

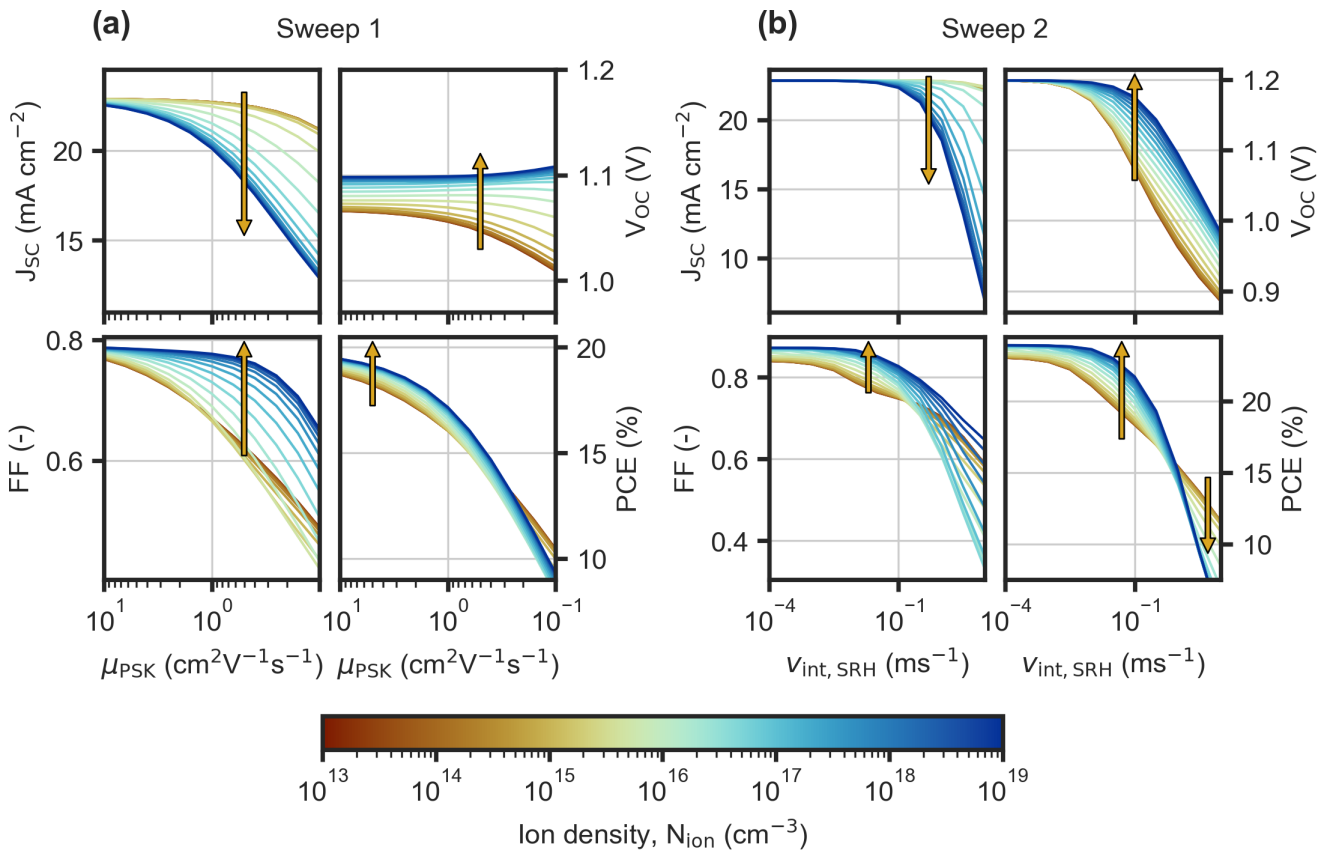

Figure S 2: Simulation for PSC with energy offset at CTLs and lower V_{bi}. Simulated stabilized J-V performance metrics with varying N_{ion}, where the arrows show the trend with increasing N_{ion}. In this model the 'ion-free' voltage, where the absolute net ionic charge reaches a minimum, is 0.85 V. (a) Bulk transport-limited device, where the recombination rates are kept constant and only the mobility of electrons and holes in perovskite (μ_{PSK}) is varied. (b) Device limited by the interfaces, where only $v_{int,SRH}$ is varied with N_{ion}.